

THE X-RAY SPECTRUM OF THE COOLING-FLOW QUASAR H1821+643 : A MASSIVE BLACK HOLE FEEDING OFF THE INTRACLUSTER MEDIUM

CHRISTOPHER S. REYNOLDS^{1,2}, ANNE M. LOHFINK^{1,3}, ARIF BABUL⁴, ANDREW C. FABIAN³, JULIE HLAVACEK-LARRONDO^{5,6,7},
HELEN R. RUSSELL³ AND STEPHEN A. WALKER³

ABSTRACT

We present a deep *Suzaku* observation of H1821+643, an extremely rare example of a powerful quasar hosted by the central massive galaxy of a rich cooling-core cluster of galaxies. Informed by previous *Chandra* studies of the cluster, we achieve a spectral separation of emission from the active galactic nucleus (AGN) and the intracluster medium (ICM). With a high degree of confidence, we identify the signatures of X-ray reflection/reprocessing by cold and slowly moving material in the AGN's immediate environment. The iron abundance of this matter is found to be significantly sub-solar ($Z \approx 0.4Z_{\odot}$), an unusual finding for powerful AGN but in line with the idea that this quasar is feeding from the ICM via a Compton-induced cooling flow. We also find a subtle soft excess that can be described phenomenologically (with an additional black body component) or as ionized X-ray reflection from the inner regions of a high inclination ($i \approx 57^{\circ}$) accretion disk around a spinning ($a > 0.4$) black hole. We describe how the ionization state of the accretion disk can be used to constrain the Eddington fraction of the source. Applying these arguments to our spectrum implies an Eddington fraction of 0.25–0.5, with an associated black hole mass of $3 - 6 \times 10^9 M_{\odot}$.

Subject headings: accretion, accretion disks — black hole physics — cooling flows — galaxies: nuclei
— X-rays: individual : H1821+643

1. INTRODUCTION

Although rare, the brightest cluster galaxies (BCGs) at the centers of cooling-core clusters of galaxies provide an important window into the physics of galaxy formation. Most of the baryons in galaxy clusters reside in the hot intracluster medium (ICM) that produces an approximately hydrostatic atmosphere in the gravitational potential of the cluster. The core of the ICM in 50% of galaxy clusters have radiative cooling times below 1 Gyr (Hudson et al. 2010). Unchecked, radiative losses would induce flows of cooled gas into the BCG resulting in $100 - 1000 M_{\odot} \text{ yr}^{-1}$ of star formation, far exceeding observed levels (Fabian 1994). It is now widely believed that mechanical heating of the ICM by a radio-loud active galactic nucleus (AGN) residing in the BCG is responsible for offsetting the ICM cooling, truncating the further growth of the BCG (Peterson & Fabian 2006; Fabian 2012). This conclusion is motivated by the fact that a very large fraction of BCGs in cool-core clusters host modest-power radio-loud AGN (Burns 1990), and that imaging X-ray observations show clear signs of interaction between these AGN jets and the

ICM (Fabian et al. 2000; Heinz et al. 2002; Bîrzan et al. 2004).

The most puzzling aspect of this AGN/ICM-feedback picture is the fueling of the AGN — how does the AGN fueling rate (determined by conditions on parsec scales) lock into the right range required to offset radiative losses on the scale of the cluster core (10–100 kpc)? Are there systems where this regulatory feedback loop breaks down? If so, what is their nature?

Here, we study one such system where a stable AGN/ICM feedback may have broken down, at least temporarily and possible for an extended period. H1821+643 ($z = 0.297$) is an extremely rare example of a luminous broad-line quasar residing in the BCG of a rich cluster — the only other comparable object in the local ($z < 0.5$) Universe is the obscured quasar IRAS 09104+4109 (O'Sullivan et al. 2012). Despite being classified as radio-quiet, H1821+643 is surrounded by a 300 kpc FRI-type radio-structure suggesting either unusual jet activity in this optically-luminous quasar or a relic from a recent radio-galaxy phase. H1821+643 shows no evidence for outflows in either *Chandra* grating studies (Fang et al. 2002; Mathur, Weinberg & Chen 2003) or FUSE UV spectroscopy (Oegerle et al. 2000).

The ICM around H1821+643 was first clearly resolved by ROSAT (Hall, Ellingson & Green 1997), but detailed study had to wait for *Chandra*. Russell et al. (2010) analyzed a moderately-deep *Chandra* exposure and, by carefully accounting for the (instrumentally) scattered emission from the quasar, showed that this is indeed a classical cool core cluster with temperature dropping from 7–8 keV at $r = 100$ kpc down to 2–3 keV within 20 kpc. More recently, using the same data, Walker et al. (2014) show that the H1821+643 cluster possesses an anomalously low core entropy when compared with other similar mass cool-core clusters. They

chris@astro.umd.edu

¹ Department of Astronomy, University of Maryland, College Park, MD 20742-2421

² Joint Space-Science Institute (JSI), College Park, MD 20742-2421

³ Institute of Astronomy, Madingley Road, Cambridge, CB3 0HA, UK

⁴ Dept. of Physics and Astronomy, University of Victoria, Victoria, British Columbia V8P 5C2, Canada

⁵ Département de Physique, Université de Montréal, C.P. 6128, Succ. Centre-Ville, Montréal, Québec H3C 3J7, Canada

⁶ Kavli Institute for Particle Astrophysics and Cosmology, Stanford University, 382 Via Pueblo Mall, Stanford, CA 94305-4060

⁷ Department of Physics, Stanford University, 452 Lomita Mall, Stanford, CA 94305-4085

suggest that, if the quasar was even more luminous in the past, the entire ICM core within 80 kpc could have been Compton-cooled by quasar radiation. Indeed, it is possible that the current quasar ($L_{\text{bol}} \sim 2 \times 10^{47} \text{ erg s}^{-1}$) is being fed by Bondi-accretion from a Compton-cooled ICM core. Compton-cooling by the quasar radiation (with Compton-temperature $kT_C \sim 0.4 \text{ keV}$) dominates over Bremsstrahlung cooling within the central 5 kpc (Russell et al. 2010). Walker et al. (2014) suggest that systems such as H1821+643 can get locked into a Compton-cooling fed state and hence grow ultramassive ($\gtrsim 10^{10} M_{\odot}$) black holes. If correct, it represents a dramatic breakdown of the AGN/ICM-regulation picture thought to operate in most clusters.

In this letter, we present an analysis of a deep observation of H1821+643 by the *Suzaku* X-ray Observatory. Our focus is on the X-ray spectrum of the quasar itself, and builds on a body of previous work. *Ginga* was the first to detect the iron-K complex in this source (Kii et al. 1991), *ASCA* showed the complex to be broadened (Yamashita et al. 1997), the *Chandra* High Energy Gratings detected the 6.4 keV fluorescence line from the AGN Fang et al. (2002) and suggested the presence of a redshifted absorption line in the quasar spectrum (Yaqoob & Serlemitsos 2005), and finally *XMM-Newton* isolated both the cold 6.4 keV iron line and an ionized line that they tentatively associated with the ICM of the cluster (Jiménez-Bailón et al. 2007).

This Letter is organized as follows. In §2 we discuss our analysis of the *Chandra* data from which we produce an ICM spectral model. §3 presents our analysis of the *Suzaku* observation, and we discuss the astrophysical implications of our findings in §4. Conclusions are drawn in §5. Throughout this work, we assume standard *Planck* cosmology (Planck Collaboration et al. 2013). At a redshift of $z = 0.297$, this places H1821+643 at a luminosity distance of 1.59 Gpc, with a linear-angular conversion of 275 kpc per arcmin.

2. THE CHANDRA VIEW OF THE ICM

Chandra observed H1821+643 in imaging mode on four visits taken within the space of 9 days in April-2008 — these data are described in detail by Russell et al. (2010) and Walker et al. (2014) who undertake a spatially-resolved study of the ICM. Since we are interested in a global ICM spectrum over the (large) *Suzaku* extraction radius, we reanalyze the data thereby also employing the latest calibration and contaminant modeling.

The data were obtained from the *Chandra* archives and reprocessed level-2 events files were created with the most recent software and calibrations (CIAO v4.6.1 and CALDB v4.5.9). The merged 0.5–5 keV *Chandra* image is shown in Fig. 1. The image is dominated by the extended emission of the intracluster medium (ICM), although the read-out streak from the luminous central AGN is clearly visible. To obtain a global spectrum of the ICM, we extract a spectrum from a circular region of radius 200 arcsec (black circle on Fig. 1). We exclude the innermost 5 arcsec (radius) and the readout streak in order to isolate, as much as possible, the ICM spectrum from the AGN emission. Background is extracted from an annulus centered on the cluster with inner and outer radius of 200 arc sec and 240 arc sec respectively (exclud-

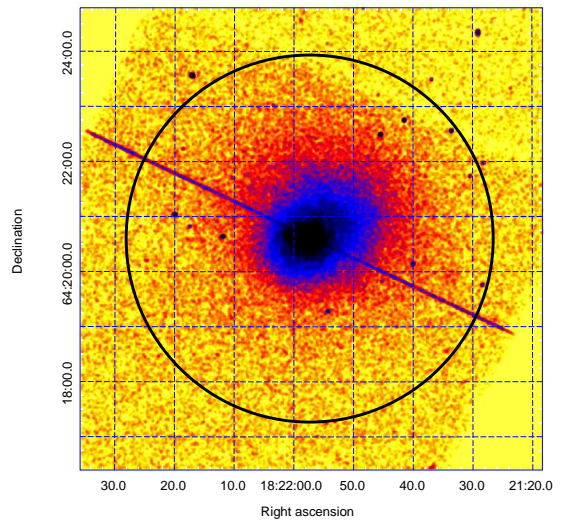


Figure 1. 0.5–5 keV *Chandra* ACIS-S3 image of H1821+643. The image is dominated by extended ICM emission. The prominent linear feature is the read-out streak from H1821+643 at the center of this cluster. The black circle shows the extraction region that is used for our *Suzaku* spectral analysis.

ing the readout streak and a bright source close to RA 18h22m17s, Dec +64d23m32s).

The resulting ICM spectrum is modeled using the XSPEC v12.8.1g package. We find that a two-temperature thermal plasma (*apec*) model modified by Galactic absorption (using *tbabs* with $N_H = 3.5 \times 10^{20} \text{ cm}^{-2}$) provides an excellent description of the spectrum. Even in this deep pointing, there are a small number of counts in the all-important iron-K band. Hence, to respect the Poisson nature of the statistics we employ the Bayesian analysis (*lstat*) capabilities of XSPEC. The resulting fit gives the two temperatures as $kT_1 = 2.0^{+2.5}_{-0.7} \text{ keV}$ and $kT_2 = 9.3 \pm 1.2 \text{ keV}$ and the (common) ICM abundance as $Z = 0.20 \pm 0.05 Z_{\odot}$. The higher temperature component strongly dominates at all energies. The total 0.5–10 keV (rest frame) luminosity of the ICM is $2.55 \times 10^{45} \text{ erg s}^{-1}$.

3. A SUZAKU STUDY OF THE AGN SPECTRUM

Suzaku has observed H1821+643 on three occasions. Here, we focus on the two observations from April-2013 that essentially form a single quasi-continuous stare with total XIS good exposure time of 375 ks (ObsIDs 708037010, 708037020). Data from all three operating XISs (XIS0, XIS1 and XIS3) were reprocessed and subjected to standard screening criteria using the *aepipeline* tool within the HEASOFT v6.15.1 suite. From the cleaned data, XIS spectra and lightcurves were extracted from a 200 arcsec radius circular aperture centered on H1821+643. Background spectra and lightcurves were extracted from source free regions around the edges of the XIS chips. No time variability of the source was found in any of the detectors and hence our discussion will address exclusively the spectral domain.

To maximize our flexibility to handle calibration issues, we do not combine XIS spectra. We jointly fit six

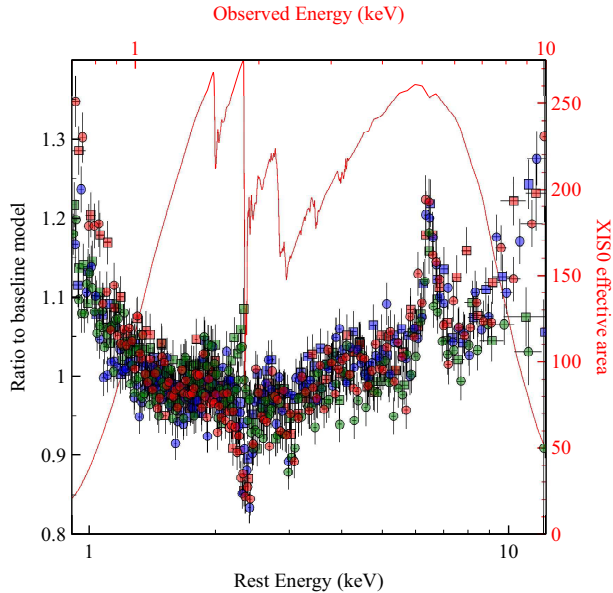


Figure 2. Ratio of XIS spectra to a baseline model consisting of ICM (fixed to *Chandra* derived parameters) and the best-fitting simple power-law. Data are shown separately for the three XIS (red=XIS0, green=XIS1, blue=XIS3) and two ObsIDs (circles=Obs708037010, squares=708037020). Comparison with the XIS0 effective area curve (red thin line) reveals that the sharp features bracketing 2 keV (observed) are very likely calibration in nature.

XIS spectra (XIS0/XIS1/XIS3 spectra from each of the two ObsIDs) in the spectral range 0.7–10 keV (observed frame). We also permit multiplicative offsets between different instruments to allow for flux-calibration errors.

Initially, we fit the XIS spectra with a model consisting of the two-temperature ICM component derived from the *Chandra* analysis (§2) and an additional power-law (PL) component to present the AGN primary continuum. Figure 2 shows the ratio of the data to this model (with best-fitting photon index $\Gamma = 2.03$). Several features of this fit are immediately apparent. Firstly, there is a strong and unmodeled iron-K α emission line at 6.4 keV. Note that this is in addition to the Fe25-K α and Fe26-K α lines associated with the ICM that are accounted for in the spectral model and hence do not show up in this ratio plot. Secondly, the spectrum has unmodeled curvature, with residuals indicating both a soft excess below 1 keV and a hard tail above 8 keV (energies quoted in rest-frame of H1821+643). Thirdly, there are clear calibration issues — there are residuals at the 10% level at energies coincident with the Silicon (detector) edge at 1.8 keV and the Gold (mirror) edge at 2.2 keV, indicating gain shifts in the detectors. Furthermore, the XIS0 is discrepant at the softest energies and XIS1 is discrepant at the highest energies, again possibly due to gain shifts.

The 6.4 keV emission line is a signature of reflection/reprocessing of the primary hard X-ray continuum by cold, optically-thick material close to the AGN. Hence, to our spectral model, we add a neutral and slow-moving X-ray reflection (REFL) component described using the *pexmon* model of Nandra et al. (2007). We also permit the instrumental gain parameters to be fit parameters in an attempt to “self-calibrate” the data. Furthermore, acknowledging that the *Chandra* calibration

may not be perfect, and the *Suzaku* point spread function mixes emission from different spatial regions of the cluster, we are conservative and permit the temperature, abundance and normalization of the dominant (~ 9 keV) ICM component to freely fit.

This model (ICM+PL+REFL) is a much better description of the data (Table 1). The cold X-ray reflection accounts for the 6.4 keV iron line and much of the hard tail, and small but significant ($< 2\%$) gain shifts largely remove the calibration residuals at the silicon and gold edges and bring the different XIS detectors into agreement with each other across the energy band. While the amplitude of the reflection is similar to that seen in many AGN (with a reflection fraction of $\mathcal{R} = 1.4$), the fit demands sub-solar iron abundance for the X-ray reprocessing circumnuclear matter ($Z_{\text{Fe}} \approx 0.4 Z_{\odot}$; this is driven by the relative strength of the iron line to the hard tail). Disaggregating the reflection component into an iron line (modeled with a Gaussian) and the Compton reflection continuum (modeled using the *pexrav* code, Magdziarz & Zdziarski 1995), we find a line energy consistent with cold iron-K α fluorescence (6.40 keV) that is marginally resolved ($\sigma \approx 60^{+35}_{-14}$ eV corresponding to a full-width half-maximum [FWHM] velocity of 6600^{+3800}_{-2500} km s $^{-1}$). This disaggregated model (ICM+PL+LINE+HUMP) permits unphysical degrees of freedom, explaining the slight discrepancy in the values of \mathcal{R} and Z_{Fe} as compared with the ICM+PL+REFL fit (Table 1). Still, the need for sub-solar abundances is clear from both the form of the Compton hump and the low equivalent width of the iron line.

This fit still leaves a subtle unmodeled soft-excess below 1 keV. This cannot be due to an additional low-temperature ICM component as the required normalization of such a component would strongly conflict with our *Chandra* spectrum as well as requiring unphysical emission measures. Phenomenologically, the soft excess can be described by a black-body (BBOD in Table 1) with rest-frame temperature $kT_{\text{bb}} \approx 80$ eV ($T_{\text{bb}} = 9.3 \times 10^5$ K). However, the physical origin of such a component (which would dominate the unabsorbed 0.1–10 keV luminosity) is unclear given that, even assuming a maximally spinning black hole, the innermost regions of the accretion disk will have temperature $T_{\text{bb}} \lesssim 3 \times 10^5$ K (Shakura & Sunyaev 1973). We note that our conclusions regarding the low-abundance of the X-ray reflector is unaffected by the inclusion of this phenomenological soft-excess.

Instead, we suggest that the soft excess arises by reflection from the inner/relativistic regions of an ionized accretion disk. We add this component to the spectral model, employing the *relxill_lp* code (García et al. 2014) which describes the relativistically blurred reflection spectrum from a geometrically-thin disk around a Kerr black hole illuminated by an X-ray “lamp-post” on the black hole spin axis at height h . Following Reynolds et al. (2012), we assume that the inner accretion disk shares the same metallicity as the other circumnuclear reflecting gas. Adding the disk reflection leads to a further highly significant improvement in the fit (Table 1). This model (ICM+PL+REFL+DISK) is shown against the (back-illuminated) XIS data in Fig. 3 (left). Figure 3 (right) illustrates how the superior sensitivity

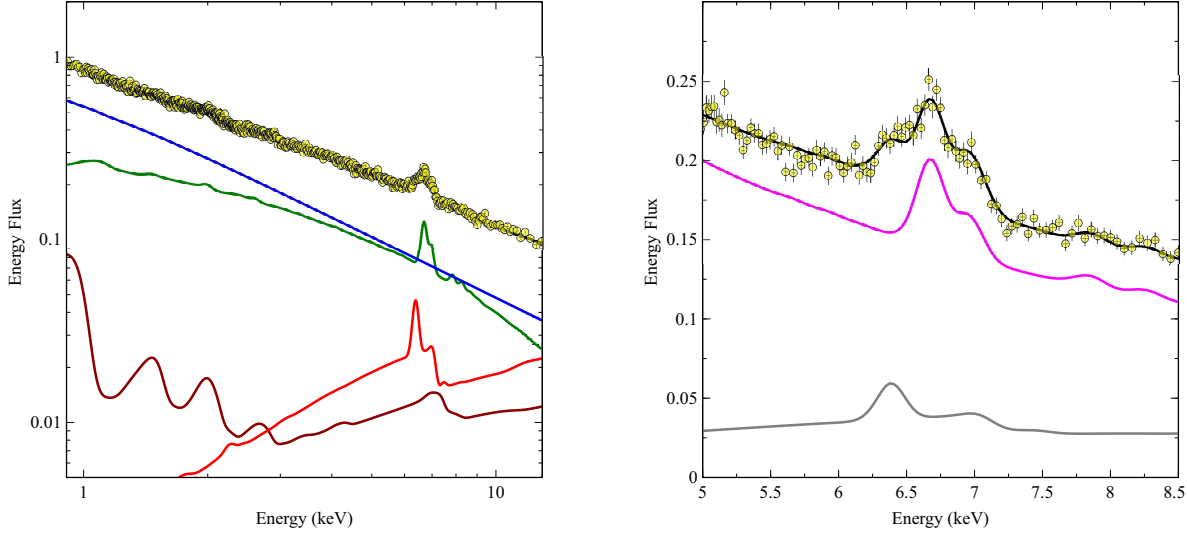


Figure 3. *Left panel* : Effective-area corrected XIS0+XIS3 spectra together with our final spectral model (ICM+PL+REFL+DISK). Coloring of model decomposition (from top to bottom); blue=PO, green=ICM, red=REFL, brown=DISK. For plotting purposes (but not for fitting), the spectra from these two backside-illuminated XISs have been combined. *Right panel* : Zoom-in on the iron line complex, breaking out the contribution from AGN reflection (grey=REFL+DISK) from the other components (magenta=ICM+PO).

Spectral Model	Parameters	χ^2/dof
ICM+PL*	$\Gamma = 2.03 \pm 0.01$	11365/7795 (1.46)
ICM+PL+REFL	$kT_2 = 8.4^{+0.5}_{-0.3}$ keV, $Z_{\text{Fe,ICM}} = 0.27 \pm 0.03 Z_{\odot}$ $\Gamma = 2.08^{+0.02}_{-0.05}$, $\mathcal{R}_{\text{cold}} = 1.37^{+0.27}_{-0.23}$, $Z_{\text{Fe,REFL}} = 0.39^{+0.03}_{-0.06}$	8302/7778 (1.067)
ICM+PL +LINE+HUMP	$kT_{\text{ICM}} = 8.75^{+0.20}_{-0.25}$, $Z_{\text{Fe,ICM}} = 0.36^{+0.03}_{-0.05}$ $E_{\text{line}} = 6.41 \pm 0.02$ keV, $\sigma_{\text{line}} = 60^{+35}_{-14}$ eV, $W_{\text{line}} = 46^{+10}_{-7}$ eV $\Gamma = 2.07 \pm 0.02$, $\mathcal{R} = 0.77^{+0.07}_{-0.11}$, $Z_{\text{Fe,REFL}} = 0.12^{+0.05}_{-0.02}$	8287/7775 (1.066)
ICM+PL +REFL+BBOD	$kT_{\text{ICM}} = 8.0^{+0.4}_{-0.5}$ keV, $Z_{\text{Fe,ICM}} = 0.33^{+0.06}_{-0.04} Z_{\odot}$ $\Gamma = 2.01 \pm 0.03$, $\mathcal{R} = 1.0 \pm 0.2$, $Z_{\text{Fe,REFL}} = 0.45^{+0.11}_{-0.08} Z_{\odot}$ $kT_{\text{bb}} = 79^{+13}_{-12}$ eV	8175/7776 (1.051)
ICM+PL +REFL+DISK	$kT_{\text{ICM}} = 7.8 \pm 0.4$ keV, $Z_{\text{Fe,ICM}} = 0.20 \pm 0.02 Z_{\odot}$ $\Gamma = 2.13 \pm 0.03$, $\mathcal{R} = 1.46 \pm 0.02$, $Z_{\text{Fe,REFL}} = 0.41^{+0.11}_{-0.06} Z_{\odot}$ $i = 57 \pm 3$, $h < 11$, $r_{\text{in}} < 3.6$, $\log \xi = 1.68 \pm 0.2$, $\mathcal{R}_{\text{disk}} = 0.79^{+0.35}_{-0.12}$	8180/7773 (1.052)
ICM+PL+REFL +DISK+BBOD	$kT_{\text{ICM}} = 7.6^{+0.5}_{-0.7}$ keV, $Z_{\text{Fe,ICM}} = 0.21^{+0.03}_{-0.02} Z_{\odot}$ $\Gamma = 2.03^{+0.02}_{-0.01}$, $\mathcal{R} = 1.15^{+0.18}_{-0.35}$, $Z_{\text{Fe,REFL}} = 0.46^{+0.20}_{-0.08} Z_{\odot}$ $i = 51^{+4}_{-5}$, $h < 17$, $r_{\text{in}} < 7.0$, $\log \xi = 2.00^{+0.05}_{-0.24}$, $\mathcal{R}_{\text{disk}} = 0.41^{+0.16}_{-0.15}$ $kT_{\text{bb}} = 0.13 \pm 0.02$ keV	8142/7771 (1.048)

Table 1

Parameters for *Suzaku* spectral fits. For the first model (flagged by *), ICM parameters are fixed at those derived from *Chandra* and the gain parameters of the XISs were held fixed at default values. For the subsequent fits, the parameters (temperature, abundance and normalization) of the hot ICM component were allowed to fit freely, as were the six sets of XIS gain parameters (three XISs, two ObsIDs). Errors are quoted at the 90% confidence level for one interesting parameter.

and spectral resolution of the *Suzaku*/XIS permits the Fe25 and Fe26 ionized lines from the ICM, and the cold iron-K line from the AGN, to be distinguished.

We note that, even when the blackbody is used to describe the soft-excess, the fit is improved by the addition of the accretion disk ($\Delta\chi^2 = 33$ for 5 additional parameters; F -test null hypothesis probability of $< 10^{-5}$). The constraints on the disk parameters in this composite soft-excess model are significantly poorer, however (last model in Table 1).

4. DISCUSSION

Our *Suzaku* spectrum has permitted the cleanest isolation yet of X-ray reprocessing in the circumnuclear en-

vironment of this rare BCG-hosted quasar. We find X-ray reflection from metal-poor ($Z \approx 0.4Z_{\odot}$), cold and slow-moving ($\lesssim 10^4 \text{ km s}^{-1}$) material in the vicinity of the AGN. We also find evidence for ionized X-ray reflection by the relativistic inner regions of the accretion disk. We consider this detection of relativistic disk reflection to be tentative since it relies upon the modeling of subtle continuum curvature (i.e. soft and hard excesses) rather than, for example, an obvious broad iron line. Still, taken at face value, our fiducial model suggests moderately ionized ($\xi \sim 50 \text{ erg cm s}^{-1}$) reflection from the innermost regions ($r_{\text{in}} < 3.6r_g$) of a high inclination ($i \approx 57^\circ$) accretion disk.

The low metallicity found in H1821+643 is unusual

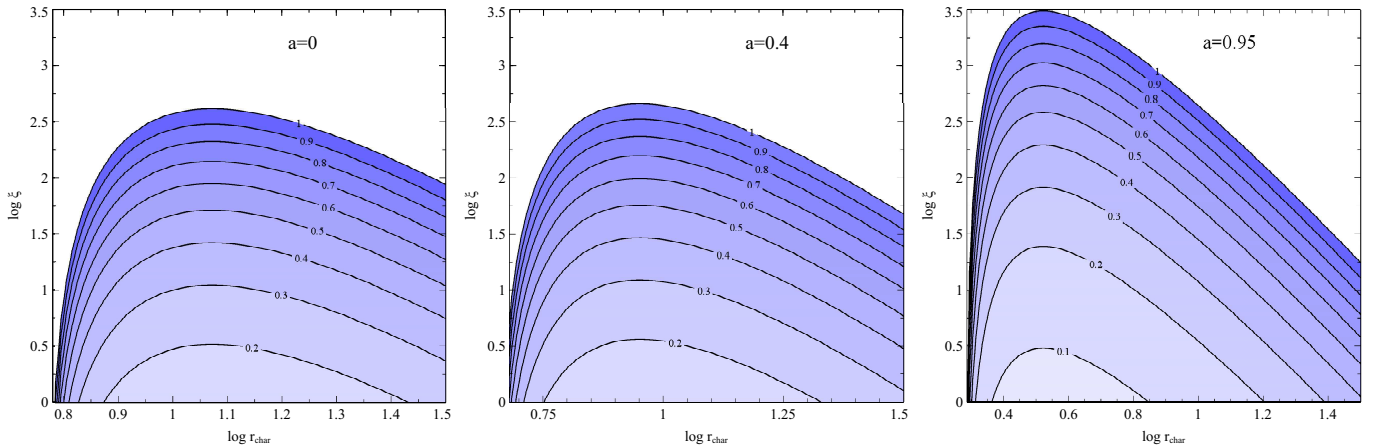


Figure 4. Contours of Eddington ratio $L_{\text{bol}}/L_{\text{Edd}}$ as functions of ionization parameter ξ and characteristic reflection radius r_{char} for three different black hole spins, based on eqn (2) of Ballantyne, McDuffie & Rusin (2011). This assumes a disk viscosity parameter of $\alpha = 0.1$, an X-ray corona that radiates $f = 0.1$ of the locally dissipated energy (although the result is very insensitive for $f = 0.1 - 0.5$), and a radiative-efficiency corresponding to the binding energy at the ISCO.

compared with other well-studied AGN. For example, it is lower by a factor of two than any of the (local) AGN studied in the *Suzaku* sample studies of Walton et al. (2013) or Patrick et al. (2012). This places constraints on the amount of star formation in the reservoir fueling this AGN that may be difficult to satisfy if the quasar is fueled by atomic or molecular gas. We note that Aravena et al. (2011) has found significant amounts ($10^{10} M_{\odot}$) of off-nuclear molecular gas in the core of this cluster, but no molecular gas has been detected in the nucleus (Combes et al. 2011). The observed AGN metallicity is consistent, however, with accretion from the ICM itself as posited in the Compton-cooled ICM fueling scenario (Russell et al. 2010; Walker et al. 2014). Russell et al. (2010) show that the core regions of the ICM have an iron abundance of $Z \sim 0.4Z_{\odot}$, the same as in the circumnuclear gas. Furthermore, the inflowing ICM will be locked into the Compton-temperature of the quasar within about 5 kpc (Russell et al. 2010) provided that the density profile is shallower than $\rho(R) \propto R^{-2}$, preventing any fragmentation and star formation. Of course, in order to produce the observed X-ray reflection signatures, some of this gas must cool within the immediate vicinity of the AGN. This likely occurs due to self-shielding from the AGN radiation in a Compton-thick circumnuclear torus or outer accretion disk.

Under the assumption that the soft-excess is solely due to ionized disk reflection, our modeling sets some interesting constraints on fundamental parameters of this AGN. If we naively identify r_{in} with the innermost stable circular orbit (ISCO), our upper limit of $r_{\text{in}} < 3.6r_g$ implies a lower limit on the black hole spin of $a > 0.65$. In fact, for the Eddington ratios likely applicable to H1821+643 (see below), the finite-thickness of the accretion disk may allow the reflecting region of the disk to penetrate somewhat into the ISCO (Reynolds & Begelman 1997); assuming a disk-thickness of $h \sim r_g$ softens our spin constraint to $a \gtrsim 0.4$ (see Fig. 5 of Reynolds & Fabian 2008).

Although model dependent, we can also estimate the Eddington fraction ($L_{\text{bol}}/L_{\text{Edd}}$) of H1821+643 from ionization state characterizing disk reflection. This issue has been examined by Ballantyne, McDuffie & Rusin

(2011) who employed the standard radiation-dominated Novikov & Thorne (1973) disk model to connect the disk ionization parameter through the disk density to the Eddington fraction. In Fig. 4 we use eqn. (2) of Ballantyne, McDuffie & Rusin (2011) to calculate the Eddington fraction as a function of disk ionization and the characteristic radius of the disk reflection r_{char} (i.e. the radius dominating the observed signal). To apply this to H1821+643 (with $\log \xi = 1.7$), we take r_{char} to be bracketed by the ISCO and our upper limit on the height of the illuminating source ($< 11r_g$). We see from Fig. 4 that, unless r_{char} is very close to the ISCO, the measure ionization implies $L_{\text{bol}}/L_{\text{Edd}} \sim 0.5$. We note Ballantyne, McDuffie & Rusin (2011) assume that the density of the disk atmosphere is the same as the mid-plane. Any tapering of density into the disk atmosphere will lead to a decrease of the inferred Eddington fraction for a given pair of observables (ξ, r_{char}). A full calibration of this will require global radiation-pressure dominated magnetohydrodynamic (MHD) accretion disk simulations, but photospheric densities are plausibly an order of magnitude lower than mid-plane densities (Reynolds & Fabian 2008) resulting in a revised constraint on the Eddington fraction of $L_{\text{bol}}/L_{\text{Edd}} \sim 0.25$. With $L_{\text{bol}} \approx 2 \times 10^{47} \text{ erg s}^{-1}$ (Russell et al. 2010), our estimated Eddington fraction of $L_{\text{bol}}/L_{\text{Edd}} \approx 0.25 - 0.5$ implies a black hole mass of $M_{\text{BH}} \approx 3 - 6 \times 10^9 M_{\odot}$. Using the parameters from Russell et al. (2010), the Bondi accretion rate corresponding to this mass is $10 - 30 M_{\odot} \text{ yr}^{-1}$, close to that needed to power this AGN.

5. CONCLUSIONS

Suzaku and *Chandra* have provided a unique glimpse into the workings of this rare BCG-hosted quasar, allowing us to isolate the spectral signatures of the AGN from those of the ICM. X-ray reflection signatures reveal a sub-solar circumnuclear environment for this AGN, consistent with a picture whereby this quasar is accreting the ICM via a Compton-cooling driven cooling flow. We also find a soft excess that can be described phenomenologically (with an ad-hoc black-body component) or as ionized reflection from the inner accretion disk. Taking the accretion disk solution suggest a lower-limit to the black hole spin of $a > 0.4$ and an Eddington fraction of

$L_{\text{bol}}/L_{\text{Edd}} \approx 0.25 - 0.5$.

If quasar Compton-cooling is really responsible for the depressed entropy profile of the ICM core (Walker et al. 2014), the quasar would have had to have undergone an past outburst with $L_{\text{bol}} \approx 4 \times 10^{48} \text{ erg s}^{-1}$. To respect the Eddington limit during this outburst, Walker et al. (2014) argue that H1821+643 may possess an ultra-massive black hole, with $M_{\text{BH}} \sim 3 \times 10^{10} M_{\odot}$. Our result suggests a slightly less massive black hole ($M_{\text{BH}} \approx 3 - 6 \times 10^9 M_{\odot}$), necessitating the outburst of H1821+643 to have been super-Eddington by a factor of $\sim 5 - 10$. Our mass estimate is significantly higher than that of Dasyra et al. (2011), $M \approx 1 \times 10^9 M_{\odot}$, based upon infrared emission line correlations. It is maybe not surprising that H1821+643 does not follow normal emission line correlations given its unusual character.

ACKNOWLEDGMENTS

We thank Eric Miller for invaluable advice and discussions about XIS contamination and calibration. CSR acknowledges support from the NASA-ADAP (grant NNX14AF86G), and AB from NSERC Discovery Grant Program.

REFERENCES

- Aravena, M., Wagg, J., Papadopoulos, P. P., & Feain, I. J., 2011, *ApJ*, 737, 64
- Ballantyne, D. R., McDuffie, J. R., & Rusin, J. S., 2011, *ApJ*, 734, 112
- Birzan, L., Rafferty, D. A., McNamara, B. R., Wise, M. W., & Nulsen, P. E. J., 2004, *ApJ*, 607, 800
- Burns, J. O., 1990, *AJ*, 99, 14
- Combes, F., García-Burillo, S., Braine, J., Schinnerer, E., Walter, F., & Colina, L., 2011, *A&A*, 528, A124
- Dasyra, K. M., Ho, L. C., Netzer, H., Combes, F., Trakhtenbrot, B., Sturm, E., Armus, L., & Elbaz, D., 2011, *ApJ*, 740, 94
- Fabian, A. C., 1994, *ARA&A*, 32, 277
- Fabian, A. C., 2012, *ARA&A*, 50, 455
- Fabian, A. C., et al., 2000, *MNRAS*, 318, L65
- Fang, T., Davis, D. S., Lee, J. C., Marshall, H. L., Bryan, G. L., & Canizares, C. R., 2002, *ApJ*, 565, 86
- García, J., et al., 2014, *ApJ*, 782, 76
- Hall, P. B., Ellingson, E., & Green, R. F., 1997, *AJ*, 113, 1179
- Heinz, S., Choi, Y.-Y., Reynolds, C. S., & Begelman, M. C., 2002, *ApJ*, 569, L79
- Hudson, D. S., Mittal, R., Reiprich, T. H., Nulsen, P. E. J., Andernach, H., & Sarazin, C. L., 2010, *A&A*, 513, A37
- Jiménez-Bailón, E., Santos-Lleó, M., Piconcelli, E., Matt, G., Guainazzi, M., & Rodríguez-Pascual, P., 2007, *A&A*, 461, 917
- Kii, T., et al., 1991, *ApJ*, 367, 455
- Magdziarz, P., & Zdziarski, A. A., 1995, *MNRAS*, 273, 837
- Mathur, S., Weinberg, D. H., & Chen, X., 2003, *ApJ*, 582, 82
- Nandra, K., O'Neill, P. M., George, I. M., & Reeves, J. N., 2007, *MNRAS*, 382, 194
- Novikov, I. D., & Thorne, K. S., 1973, in *Black Holes (Les Astres Occlus)*, ed. C. Dewitt, B. S. Dewitt, 343
- Oegerle, W. R., et al., 2000, *ApJ*, 538, L23
- O'Sullivan, E., et al., 2012, *MNRAS*, 424, 2971
- Patrick, A. R., Reeves, J. N., Porquet, D., Markowitz, A. G., Braitto, V., & Lobban, A. P., 2012, *MNRAS*, 426, 2522
- Peterson, J. R., & Fabian, A. C., 2006, *Phys. Rep.*, 427, 1
- Planck Collaboration et al., 2013, *ArXiv e-prints*
- Reynolds, C. S., & Begelman, M. C., 1997, *ApJ*, 488, 109
- Reynolds, C. S., Brenneman, L. W., Lohfink, A. M., Trippe, M. L., Miller, J. M., Fabian, A. C., & Nowak, M. A., 2012, *ApJ*, 755, 88
- Reynolds, C. S., & Fabian, A. C., 2008, *ApJ*, 675, 1048
- Russell, H. R., Fabian, A. C., Sanders, J. S., Johnstone, R. M., Blundell, K. M., Brandt, W. N., & Crawford, C. S., 2010, *MNRAS*, 402, 1561
- Shakura, N. I., & Sunyaev, R. A., 1973, *A&A*, 24, 337
- Walker, S. A., Fabian, A. C., Russell, H. R., & Sanders, J. S., 2014, *ArXiv e-prints*
- Walton, D. J., Nardini, E., Fabian, A. C., Gallo, L. C., & Reis, R. C., 2013, *MNRAS*, 428, 2901
- Yamashita, A., Matsumoto, C., Ishida, M., Inoue, H., Kii, T., Makishima, K., Takahashi, T., & Tashiro, M., 1997, *ApJ*, 486, 763
- Yaqoob, T., & Serlemitsos, P., 2005, *ApJ*, 623, 112